RSC Advances

ARTICLE

Received 00th January 20xx,
Accepted 00th January 20xx
DOI: 10.1039/x0xx00000x
www.rsc.org/

In, V-codoped TiO_2 Nanocomposite Prepared via Photochemical Reduction Technique as Novel High Efficient Visible-Light-Driven Nanophotocatalyst

V. Jabbari [a*], M. Hamadanian [b,c**], A. Reisi-Vanani [c], P. Razi [c], S. Hoseinifard [c], D. Villagrán [a]

Abstract

In the current study, a series of novel and high efficient photocatalysts of In, V-codoped TiO_2 were developed. The TiO_2 nanoparticles were synthesized by sol–gel and hydrothermal methods and then different molar percentage (0.1-1%) of vanadium (V) and Indium (In) nanoclusters were deposited over TiO_2 nanoparticles via photochemical reduction. XRD, SEM, EDX, TEM, XPS and UV-Vis DRS analysis were carried out to characterize the prepared In, V-codoped TiO_2 nanocatalysts and methyl orange (MO) was used as probe environmental pollutant to test the photocatalytic performance of the prepared catalysts under UV and visible light irradiation. Our findings demonstrated that In and V nanoclusters were successfully deposited over TiO_2 particles via photochemical deposition technique and the metal doping slightly suppressed TiO_2 crystal growth. The optical analysis showed a red shift in light absorption spectrum and decreases in band gap of In, V-codoped TiO_2 catalysts compared to that of parent TiO_2. XPS study revealed that the doped elements of In and V are in oxidation state of 3 (In^{III}), 4 (V^{IV}) and 5 (V^{V}), respectively. The photo-oxidative decomposition of MO showed that doping of In and V can considerably improve photocatalytic activity of TiO_2. Thus, for the first time, we have demonstrated that TiO_2 codoped with binary metals of In and V can serve as high efficient visible-light-active photocatalyst.

Keywords: In, V-codoped TiO_2; Nanoparticles; Photodeposition; Photocatalytic activity

1. Introduction

In the recent years, many attempts has been devoted to developing a heterogeneous photocatalysts with high activity for the environmental applications, including water disinfection, water purification, air purification and hazardous waste remediation [1, 2]. Among the various metal oxide semiconductor photocatalysts, TiO_2 has shown to be the most suitable for environmental purposes due to its strong oxidizing power, chemical inertness, long-term stability, and cost effectiveness [3, 4]. The primary event occurring on the TiO_2 surface after irradiation is generation of electrons (e_{cb}^-) and holes (h_{vb}^+). In these reactions, the organic pollutants are oxidized (decomposed) by the photo-generated h_{vb}^+ or by the reactive oxygen species ($OH^{\bullet}$ and O_2^- radicals) formed onto the illuminated TiO_2 surface. However, the practical application of TiO_2 is limited by two main factors: first, due to wide band gap of TiO_2 (3.2 eV for anatase, 3.0 eV for rutile phase) [5], it is can only absorb UV portion of solar light (λ<387 nm) which is up to 5% of solar light [6]. Therefore, in order to extend its practical application, many efforts have been made to design second-generation TiO_2-based photocatalysts which would be able to induce photocatalysis under visible light irradiation. Secondly, the low rate of photocatalytic decomposition using TiO_2 photocatalyst is attributed to the charge recombination of photogenerated electron-hole pairs (charge carriers).

[a.] Department of Chemistry, The University of Texas at El Paso, El Paso, Texas 79968, USA.
[b.] Institute of Nanosciences and Nanotechnology, University of Kashan, Kashan, IRAN
[c.] Department of Physical Chemistry, Faculty of Chemistry, University of Kashan, Kashan, IRAN.
Corresponding author(s); Tel +98 31 55912382; Fax +98 31 55912397; P.O. Box 87317-51167. Email: hamadani@kashanuac.ir (M. Hamadanian) and vjabbari86@gmail.com & vahid_jabbari.azeri@yahoo.com (V. Jabbari).

In order to overcome these problems, several approaches have been proposed: metal doping [7, 8], metal ion doping [9-11], nonmetal doping [12-14], dye-sensitizing of TiO_2 (e.g. thionine) [15, 16], making composites of TiO_2 with other semiconductor owning narrow band gap energy (e.g. CdS particles) [17], and doping TiO_2 with up-conversion luminescence agent [18]. Among them, metal doping has been proved to be a very promising approach due to greatly extending the light absorption of TiO_2 and significantly improving the trapping efficiency of change carriers [19-22].

Raftery et al., reported that doping of TiO_2 nanoparticles with vanadium cations could extend the photoresponse of TiO_2 to visible light region (396–450 nm) and also temporarily trap the photogenerated electrons (e^-) and holes (h^+), and thus suppress the charge recombination of the charge carriers [23]. Wu and Chen found that V-doped TiO_2 exhibits photoactivity in visible light region and show a “red shift” in the UV–Vis spectra [24]. Choi et al., reported that doping of V^{4+} into TiO_2 at V/Ti ratio of 0.1–0.5 %wt, can significantly increase the TiO_2 photoreactivity due to the improved interfacial charge transfer [25].

Wang et al., observed that by introducing In ions into TiO_2 structure, not just new energy states emerge between the TiO_2 band gap which results in considerable red-shift in absorption, but also the ions facilitate the charge separation [26]. The same results were reported by other group [27]. They analyzed the photocatalytic activity of In-doped TiO_2 under visible light illumination. It was demonstrated that the In doping improve visible light response of TiO_2 catalyst and enhance the charge carriers separation, which the factors combined leads to the significant improvement in photocatalytic performance of TiO_2 under visible light illumination.

Modification of TiO_2 by binary doping of metal ions is a novel process for enhancing the optical efficiency of TiO_2. The synergic effect of codoping can further improve the photocatalytic activity of

TiO_2. Recently, a number of literatures have reported different types of photocatalysts using binary metal-doped TiO_2. Estrellan et al. synthesized Fe, Nb-codoped TiO_2 via sol-gel method [28]. Fe-Nb-TiO_2 exhibited anatase crystalline phase with high value of crystallinity along with red shift in light absorption. It was reported that TiO_2 co-doping with cation pairs of Rh^{3+}/Sb^{5+} can result in greatly improved photocatalytic activity [29]. Zhang et al., prepared V, Sc-codoped TiO_2 by sol-gel method and they found that binary doping of these metals led to considerable decline in the charge recombination and also the doping induce a large red shift in the TiO_2 absorption spectrum [30].

Photochemical reduction method have recently attracted many attentions due to its versatile advantages: (i) controlled reduction of metal ions can be carried out without using the excess reducing agent, (ii) the reduction reaction is uniformly performed in the solution, and (iii) light radiation is absorbed regardless of the presence of light absorbing solutes and products [31].

The aim of the current work, which to best of our knowledge is for the first time, is to study the synergistic effect of co-doping of In and V ions on the photocatalytic activity of TiO_2 nanoparticles. The physicochemical characteristic of the prepared catalysts were investigated by XRD, SEM, EDX, TEM, XPS and UV-Vis DRS. Methyl orange (MO) was used as probe organic pollutant to monitor photocatalytic performance of the In, V-codoped TiO_2 catalysts. Finally, it is found that the In, V-codoped TiO_2 shows size in nanometer range with strong light absorbance and high quantum efficiency of charge carriers and the 0.2In-0.2V/TiO_2 catalyst exhibited superior photocatalytic activity compared to parent TiO_2, under UV and visible light irradiation.

2. Experimental

2.1. Chemicals

Titanium(IV) tetraisopropoxide (TTIP, $Ti[OCH(CH_3)_4]_4$ (Merck, >98%), glacial acetic acid (Merck, >99.8%), vanadium chloride (VCl_3, Merck), and indium chloride ($InCl_3$, Merck) were used as received without further purification. Deionized water was prepared by an ultra pure water system (Smart-2-Pure, TKA Co, Germany). Methyl orange (MO, M.W. = 695.58 $gmol^{-1}$) was provided by Alvan Co, Iran.

2.2. Synthesis of Pure TiO_2 Nanoparticles by Hydrothermal and Sol-Gel

Pure TiO_2 nanoparticles were prepared according to previous studies by sol-gel [32] and hydrothermal [33] methods. TiO_2 nanoparticles prepared by hydrothermal and sol-gel processes were calcined at 450 ^oC for 3h and 500 ^oC for 2h, respectively.

2.3. Preparation of In-TiO_2 and In, V-codoped TiO_2 Nanoparticles via Photochemical Reduction

The photochemical route is a promising way to form noble metal–semiconductor nanocomposites *in situ* by reducing noble metal ions adsorbed on the surface of a semiconductor. It is well known that a semiconductor can be excited and then generate electrons (e^-) and holes (h^+) in the conduction band (CB) and valence band (VB), respectively, if the energy of the photons of the incident light is larger than that of band gap of the semiconductor [34]. The metal ion dopants influence the photo-efficiency of TiO_2 by acting as electron or hole trap centres within band gap of TiO_2 and alter the e^-/h^+ pair recombination rate [32], through following process. The photo-reduction of the metal ions (Eq. 1) is accompanying the elimination of photo-generated holes using water oxidation (Eq. 2):

$$M^{n+} + ne^- \rightarrow M^o \quad (1)$$

$$2H_2O + 4h^+ \rightarrow O_2 + 4H^+ \quad (2)$$

In-doped TiO_2 with various metal content were prepared as follows: To prepare In-doped TiO_2, first different molar percent of $InCl_3$ (0.1, 0.2, 0.4, 0.6, 1.0% of V to Ti molar ratio) as indium source was added to 100 ml of aqueous solution containing certain amount of pure TiO_2 particles synthesized by sol-gel and hydrothermal processes. Then, the resulting solution was purged with high-purity N_2 atmosphere while stirring. Afterward, the resulting solution was transferred to a quartz reactor with its head covered and was put under UV irradiation for 12 hours, under vigorous stirring. After this stage, the precursor was filtered by centrifugation and washed with deionized water for several times. The resulting powders were dried at 100 ^oC for 12 h.

To prepare In,V-codoped TiO_2, the same method for synthesis of In-doped TiO_2 was adopted using both $InCl_3$ (0.1, 0.2, 0.4, 0.6, 1.0% of V to Ti molar ratio) as indium source and VCl_3 (0.1, 0.2, 0.4, 0.6, 1.0% of V to Ti molar ratio) as vanadium source.

2.4. Characterization of the Prepared Catalysts

Crystalline phases of the prepared samples were analysed by X-ray powder diffractometer (XRD, Bruker D8 Discover X-ray Diffractometer). The morphology was revealed by a transmission electron microscope (TEM, Hitachi H-7650) and scanning electron microscope (SEM, Hitachi S-4800) equipped with an energy dispersive X-ray detector (EDAX). UV-Vis DRS spectra of the samples were recorded by a Shimadzu 1800 spectrometer. UV-Vis absorption spectra of MO degradation were measured by UV-Vis spectrophotometer (Perkin Elmer Lambda2S, Germany). XPS test was monitored by Omicron XPS/UPS system with Argus detector which uses Omicron's DAR 400 dual Mg/Al X-ray source.

2.5. Photocatalytic Performance Analysis

The photocatalytic activity of the prepared catalysts was analyzed by MO degradation under UV and visible lights irradiation. Each time, 0.1 gr photocatalyst was dispersed into 100 ml MO aqueous solution with a concentration of 10 mg l^{-1} held in a quartz reactor (with a dimension of 12cm × 5cm, height and diameter, respectively). Two 400W Osram lamps provided the visible and UV sources, located 40 cm and 25 cm away from the reactor, respectively. The reaction system was stirred in dark for 30min to achieve absorption equilibrium, before irradiation.

3. Results and Discussions

3.1. X-ray Diffraction Patterns

Figure 1 shows the XRD patterns of parent TiO_2 and In, V-codoped TiO_2 catalysts. (101), (004), (200), (105), (211), (204), (116) diffraction peaks were proved anatase phase for the pure TiO_2 [35]. A main peak for anatase phase around 2θ= 25.2º (101) has tetragonal form [35]. Also no rutile phase diffraction peak was detected in the samples. Furthermore, the XRD pattern did not show any In or V phase (as in metallic or metal oxide state) and it was concluded that In and V ions were uniformly loaded onto the TiO_2 surface. There is also relatively small shift in In, V-codoped TiO_2 compared to parent TiO_2, which shows slight distortion in the TiO_2 structure.

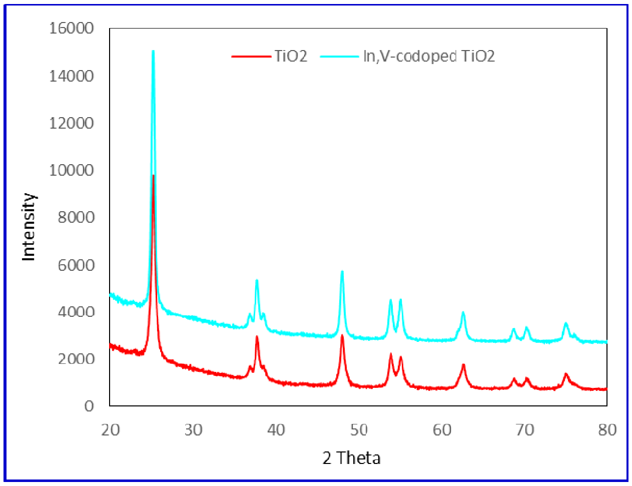

Fig. 1. XRD patterns of parent TiO_2 and In, V-codoped TiO_2 catalysts.

Debye-Scherrer formula was used for measuring the average crystallite size of the prepared catalysts as follows:

D = Kλ/β cos θ (3)

Where k is the constant which is taken as 0.9 here, λ is the wavelength of the X-ray radiation (λ= 0.1541 nm, β is the corrected band broadening [(FWHM) full-width at half-maximum] after subtraction of equipment broadening and θ is the Bragg angle [35]. By using mentioned equation on the anatase phase (2θ= 25.2, 48.2, 55.2º) the average particle size was calculated for pure TiO_2 synthesized via hydrothermal method to be about 18.75. The particle size of In, V-codoped TiO_2 with 0.2%mol metal content was estimated to be 14.3 nm. As it is obvious, we found that doping of TiO_2 by In and V ions results in decreases of TiO_2 catalyst particle size.

Indeed, the formation of Ti–O–In or Ti–O–V inhibits transition of the TiO_2 phase and blocks Ti–O species at the interface with TiO_2 domains, and thus preventing agglomeration of TiO_2 particles. Hence, doping of TiO_2 by In and V minimizes the charge carrier recombination during the photocatalytic decomposition of MO, and as results, it is expected that In, V-codoped TiO_2 show a higher photocatalytic activity compared to the pure TiO_2.

3.2. SEM-EDX Analysis

Figure 2 shows SEM micrographs of pure TiO_2 and 0.2%In-0.2%V/TiO_2 catalysts. The SEM micrographs show that the particles consist of uniform, global and slightly agglomerated particles, and the doped metal ions had not obvious influence on the morphology of the samples. Further observation indicates that the morphology of samples is very rough and maybe beneficial to enhancing the adsorption of dye due to its great surface roughness and high surface area [36]. Both narrow size distribution of nanoparticles and well dispersion are in favour of photoactivity.

The EDX measurement was carried out to verify the formation of In and V nanoclusters onto the TiO_2 surface after photochemical reduction. As it is obvious from Figure 3, new peaks are appeared in the TiO_2 spectra after metal deposition which confirms the presence of In and V in the prepared In, V/TiO_2 sample.

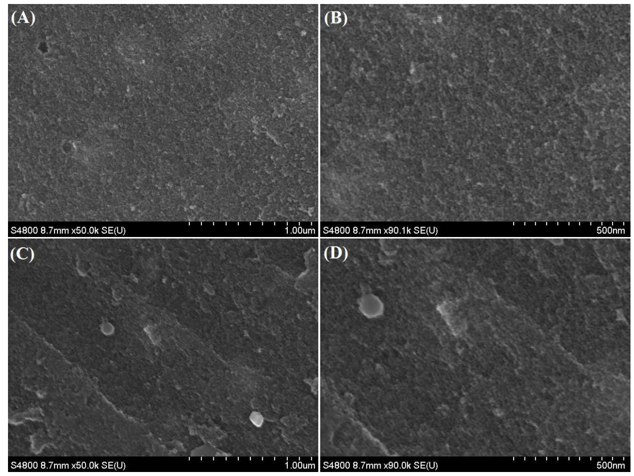

Fig. 2. SEM micrographs of pure TiO_2 (a,b) and In, V-codoped TiO_2 (c,d).

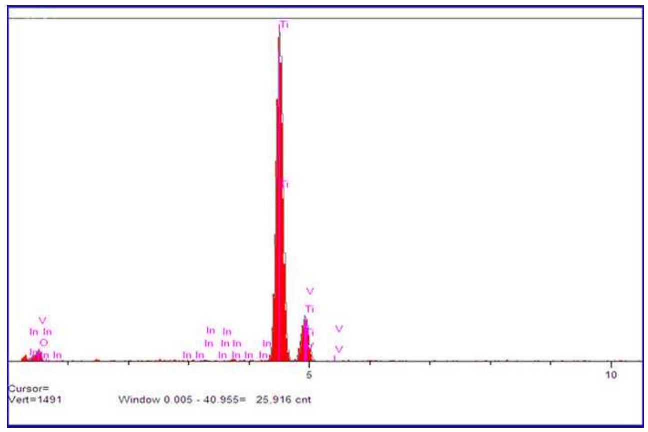

Fig. 3. EDAX result of In, V-codoped TiO_2.

3.3. TEM Analysis

TEM images of pure TiO_2 and 0.2%In-0.2%V/TiO_2 catalysts are shown in Figure 4. Based on the images, the particle size of 0.2%In-0.2%V/TiO_2 sample was estimated to be around 11-13 nm which is in a good agreement with the particle size estimated from Debye-Scherrer formula (12-15 nm). Also, HRTEM image shows that the peak located at 2theta= 25 matches well with the (101) plane of anatase TiO2 (JCPDS Card No. 01-065-9124), indicating the formation of anatase TiO2 [37].

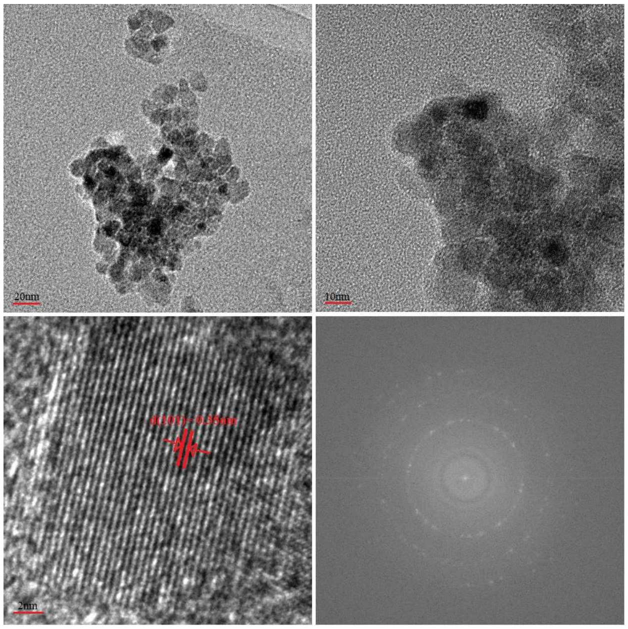

Fig. 4. HRTEM images of In, V-codoped TiO_2.

3.4. XPS Study of In, V-codoped TiO_2 Catalyst

XPS test is carried out to determine the oxidation states of In and V in In,V-codoped TiO_2 catalyst. Figure 5 shows the XPS spectrum for In 3d and V 2p of In,V-codoped TiO_2. As shown in Figure 5, XPS spectrum in Ti 2p region of In,V-codoped TiO_2 shows peaks at around 456 eV (Ti 2p3/2) and 462 eV (Ti 2p1/2), which is corresponding to Ti^{4+} ions in TiO_2 lattice [38]. The O 1s peak of the prepared In,V-codoped TiO_2 can be seen in binding energy of around 527 eV, which is attributed to crystal lattice oxygen (O^{2-}) of In,V-codoped TiO_2 (Ti–O–Ti; Ti–O–In; Ti–O–V) [38].

Our findings show that In element in In,V-codoped TiO_2 exist in oxidation state of 3, In(III), showing peaks around 444.8 eV (In $3d_{5/2}$) and 450.6 eV (In $3d_{3/2}$), which is in agreement with previous reports [39]. Regarding to presence of V element in the In,V-codoped TiO_2 catalyst, we have witnessed peak for V 2p3/2 which consists of two peaks, one at around 516 eV, related to V^{4+} and around 517 eV, related to V^{5+} [38].

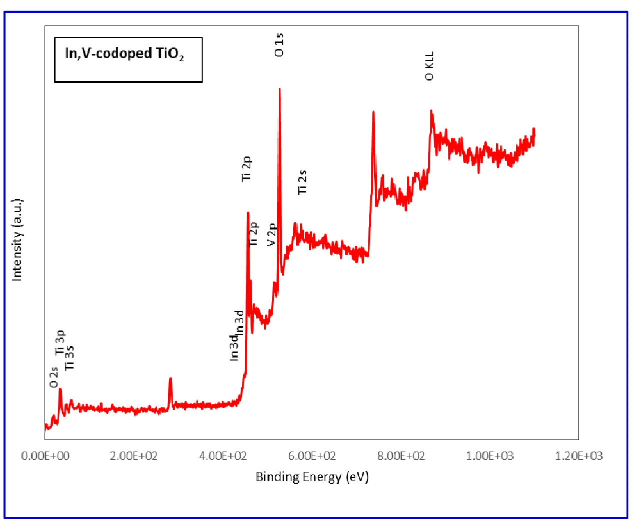

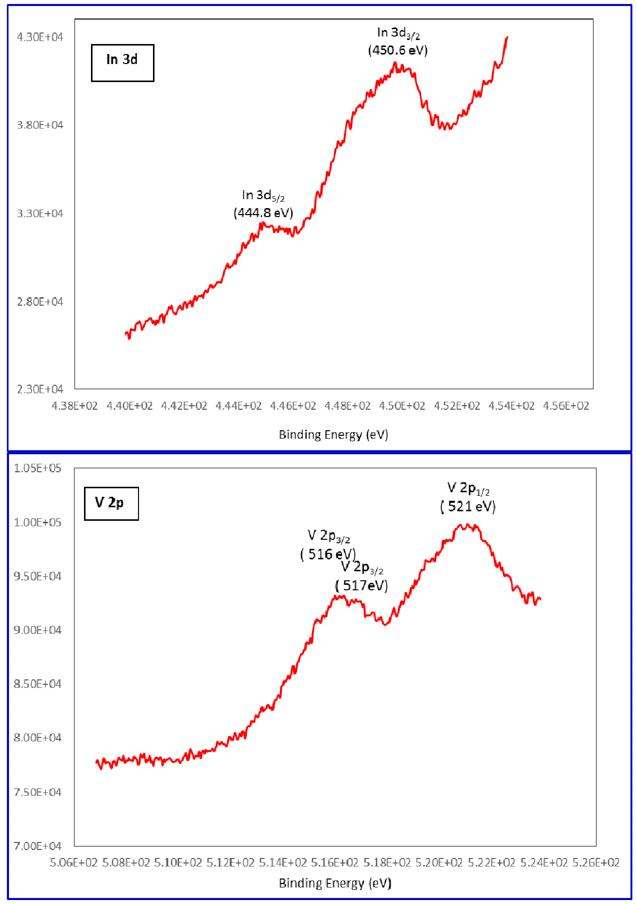

Fig. 5. XPS spectra of In, V-codoped TiO_2.

3.5. UV-Vis DRS Analysis of In, V-codoped TiO_2 Catalysts

It is well-known that the photocatalytic performance of metal oxide semiconductor is closely related to its band gap structure. The UV–Vis absorbance spectra of the pure and metal doped TiO_2 samples are shown in Figure 6. By considering the absorbance spectra of pure TiO_2, the onset of the absorption appears at 380 nm, which matches well with intrinsic band gap of the anatase TiO_2 (3.2 eV). Also, it is obvious that there is a considerable shift in the absorption toward higher wavelength for the In, V-codoped TiO_2 catalyst compared to the pure TiO_2. The reason for that might be attributed to appearance of the new electronic energy state in the middle of TiO_2 band gap, which result in gap reduction between conduction band (CB) and valence band (VB) of the TiO_2, allowing TiO_2 to absorb visible light [36].

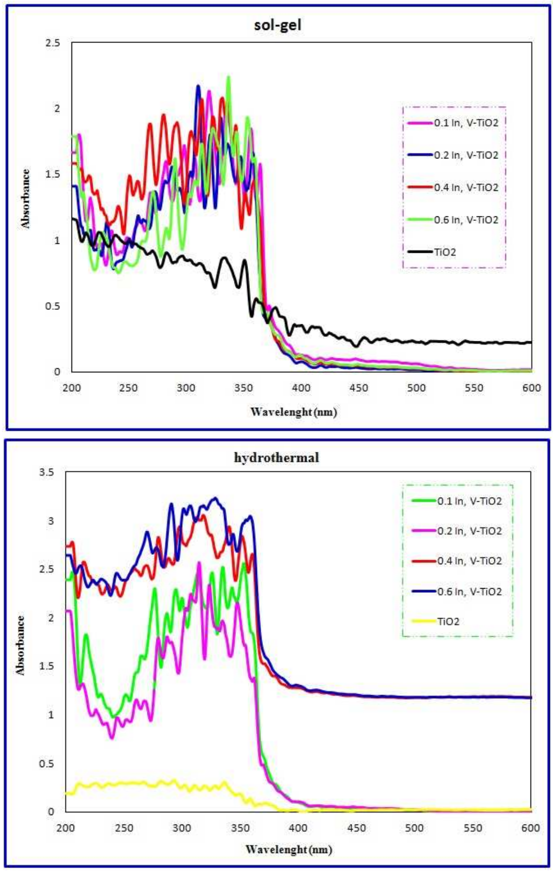

Fig. 6. UV–Vis DRS absorption spectra of as-prepared TiO_2 and In, V-codoped TiO_2 nanoparticles with different metal content.

By using the following equation, band gap values of the pure TiO_2 and In, V-codoped TiO_2 catalysts were calculated [40]:

$E_g = h \times c/\lambda$ (4)

where, E_g = band gap energy, h = Planck's constant in eV (4.135×10^{-15} eV), C = velocity of light (3×10^8 m/s), λ = wavelength of the corresponding catalysts. We found that the band gap values were lower for the doped catalysts (below 3 eV) compared to the pure TiO_2 catalyst (up to 3 eV).

Furthermore, the V 3d energy state and In 4d energy state play important roles in interfacial charge transfer and elimination of charge recombination. Thus, transition metal ions (V and In) would act as an efficient electron scavenger to trap the electrons of CB state of TiO_2 [35]. Accordingly, it can be presumed that the In, V-TiO_2 photocatalyst may demonstrate higher photocatalytic activity under visible light irradiation, compared to the pure TiO_2.

3.6. Photocatalytic Performance of In, V-codoped TiO_2 Catalysts

Methyl orange (MO) was used as probe environmental pollutant to study photocatalytic activity of the pure TiO_2 and metal-doped TiO_2 catalysts. Table 1 and Table 2 show the degradation results over In-doped TiO_2 with various metal content synthesized via hydrothermal-assisted photochemical reduction and sol-gel assisted photochemical reduction, respectively, and Figures 7 and Figures 8 demonstrate photocatalytic performance of In,V-codoped TiO_2 with various metals content synthesized via sol-gel assisted photochemical reduction and hydrothermal-assisted photochemical reduction, respectively. Before shining UV or visible light on the catalysts, the MO solution containing the catalysts were stirred in dark for half an hour. Our detection results exhibited that the MO concentration showed negligible decrease due to slight absorption on the photocatalysts surface, which showed that there was almost no MO decomposition in the absence of light irradiation.

Table 1. The photocatalytic results of MO degradation using In-doped TiO_2 nanoparticles with various In(III) content, prepared via hydrothermal assisted photochemical deposition.

UV Light Illumination				
Time (min) → Elem. (%) ↓	15	30	45	60
0	37.32	59.77	81.07	90.80
0.05	43.91	59.78	75.71	82.56
0.1	35.42	48.58	67.82	82.68
0.2	52.41	71.72	86.51	95.09
0.5	46.28	81.99	88.66	98.47
0.8	45.21	78.47	88.12	96.17
1	38.16	60.69	81.53	92.18
2	44.67	64.37	81.23	92.87

Visible Light Illumination					
Time (min) → Elem. (%) ↓	30	60	90	120	150
0	23.85	34.81	48.15	62.98	69.38
0.05	26.15	44.56	60.15	74.21	79.81
0.1	28.66	48.89	70.81	93.55	98.89
0.2	28.89	46.07	61.63	77.63	82.78
0.5	9.18	22.96	36.15	47.48	52.72
0.8	8.02	19.51	29.63	41.52	48.21
1	21.48	37.18	51.48	66.07	72.13
2	26.89	43.11	58.59	73.19	78.32

Table 2. The photocatalytic results of MO degradation using In-doped TiO_2 nanoparticles with various In(III) content, prepared via sol-gel assisted photochemical deposition.

UV Light Illumination				
Time (min) → Elem. (%) ↓	15	30	45	60
0	43.67	67.66	81.02	91.02
0.1	45.08	68.36	82.66	91.48
0.2	45.08	68.36	82.66	91.48
0.4	38.20	64.76	76.48	81.95
0.6	40.93	67.11	78.52	89.76
1	45.08	69.53	85.55	92.97
2	49.14	71.01	91.09	96.09

Visible Light Illumination					
Time (min) → Elem. (%) ↓	30	60	90	120	150
0	20	30	42.50	52.71	61.20
0.1	12.86	25.50	41.53	48.57	53.43
0.2	30.86	52.21	69.28	83.57	92.50
0.4	27.28	47.14	52.93	70.81	80.28
0.6	21.71	45.32	60.15	64.71	74.86
1	19	27.93	41.25	50.28	57.36
2	26.36	42.07	57.07	68.43	81.92

As it is apparent from Table 1, all In-doped TiO_2 nanoparticles are visible light active. The optimal dosage of indium ion to get highest photocatalytic activity for MO decomposition was found to be 0.1% (hydrothermal-assisted photodeposition) and 0.2% (sol-gel assisted photodeposition) under visible light and 0.5% (hydrothermal-assisted photodeposition) and 2% (sol-gel assisted photodeposition) under UV light illumination.

Our findings regarding to In, V-codoped TiO_2 catalyst prepared with sol-gel assisted photodeposition technique (Figures 7), illustrate no improvement in photocatalytic performance in comparison to pure TiO_2. But in case of In, V-codoped TiO_2 catalyst prepared with hydrothermal-assisted photodeposition technique (Figures 8), we found that TiO_2 catalyst with 0.2% metal content achieved the higher rates of MO decomposition compared to the pure TiO_2 catalyst. Indeed, in the In, V-codoped TiO_2 catalyst the metal could acts as electron trapper and thus reduce the charge recombination rate which is in favour of photocatalytic activity enhancement. The improvement of pollutant degradation was initially increased with the increase of metal content, but it was declined while the metal content reached a high level [41-43]. As matter of fact, in In, V-codoped TiO_2 catalysts with metal content of higher than 0.2%, the metal ions acts as electron-hole recombination center which as result decreases the photo-efficiency and photocatalytic activity.

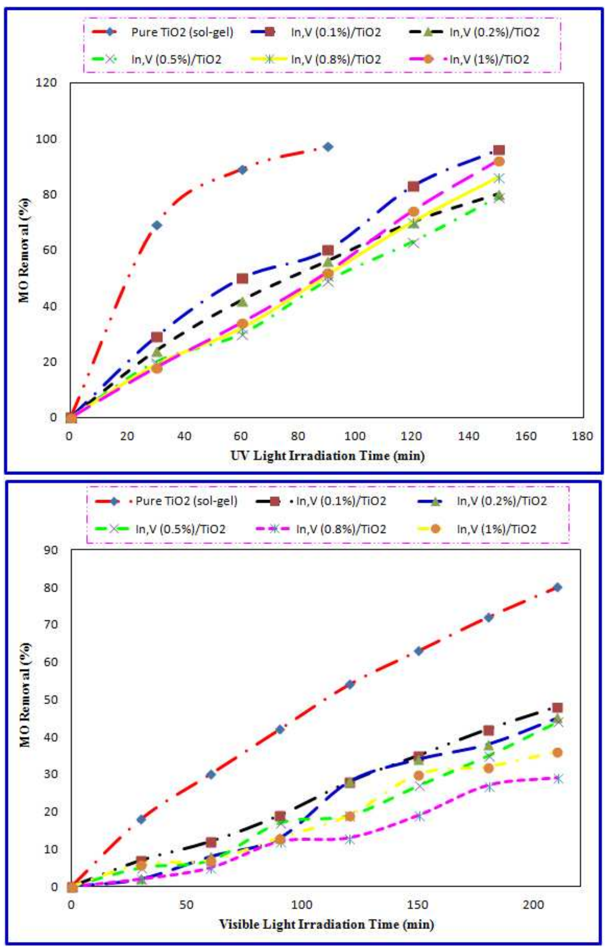

Fig. 7. Photocatalytic activity of pure TiO_2 and In, V-codoped TiO_2 catalysts prepared by sol-gel method, under UV (a) and visible light (b) irradiation.

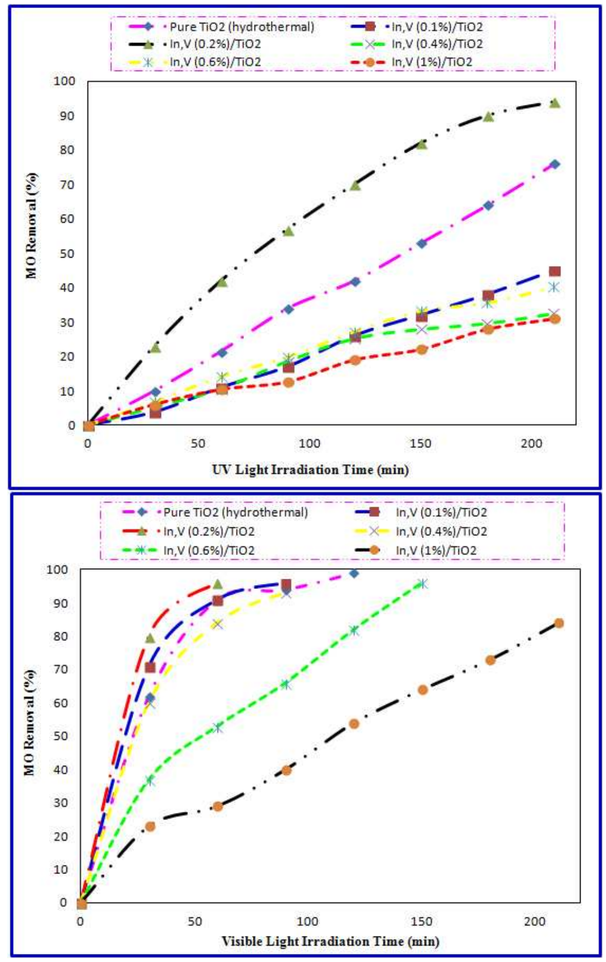

Fig. 8. Photocatalytic activity of pure TiO_2 and In, V-codoped TiO_2 catalysts prepared by hydrothermal method, under UV (a) and visible light (b) irradiation.

To investigate the In^{3+} doping effect on the photocatalytic performance of TiO_2, it was found that loading indium ions onto TiO_2 particles prevent the particle growth and In^{3+} change to In^{2+} as electron trapper by forming a low energy level between CB and VB of TiO_2. In absence of light irradiation, In^{2+} ions convert to In^{3+} and atmospheric O_2 traps released electron as electron acceptor and produce O_2^{-}. The process mechanism is shown below:

$TiO_2 + h\nu \rightarrow TiO_2^{\cdot} + e^-$ (5)

$In^{3+} + e^- \rightarrow In^{2+}$ (6)

$In^{2+} + \text{Oxidation} \rightarrow In^{3+} + e^-$ (7)

$O_2 + e^- \rightarrow O_2^{\cdot}$. (8)

In fact, this metal–TiO_2 support interface is largely beneficial for the photocatalytic reactions. The close contact of metal nanoclusters with TiO_2 nanoparticles allows the photogenerated electrons (free or trapped) in TiO_2 lattices (Eqs. (9) and (10)) to be transferred to the metal lattices (Eqs. (11) and (12)) easily;

$TiO_2 + h\nu \rightarrow e^-_{cb} + h^+_{vb}$ (9)

$Ti^{4+} + e^-_{cb} \rightarrow Ti^{3+}$ (10)

$M + e^-_{cb} \rightarrow M^-$ (11)

$Ti^{3+} + M \rightarrow Ti^{4+} + M^-$ (12)

where $h\nu$ represents the light irradiation energy, e^-_{cb} and h^+_{vb} represent the photogenerated electrons in CB and holes in the VB of TiO_2, respectively. Ti^{n+} and M_m^- represent the titanium ions or atoms in the TiO_2 crystal and metal atoms or ions in the metallic clusters, respectively.

The number of electrons in the bulk TiO_2 is reduced; thereby the possibility of recombination (Eqs. (13) and (14)) is declined:

$e^-_{cb} + h^+_{vb} \rightarrow$ recombination (13)

$Ti^{3+} + h^+_{vb} \rightarrow Ti^{4+}$ (14)

In general, most of the photogenerated electrons and holes recombine through Eqs. (13) and (14) processes, and only a small number remain for the photocatalytic reactions. By using IR spectroscopic, it was reported that electron transfer from the TiO_2 support to the deposited metal clusters is the bottleneck of the photocatalytic reactions [44].

Based on our findings, there is a significant potential to enhance efficiency of photocatalytic reactions through improving charge separation and charge transfer using proper metal nanoclusters loading over TiO_2 catalysts.

4. Conclusions

In the current study, a series of novel In, V-codoped TiO_2 catalysts with different In and V contents were synthesized by photochemical reduction technique and were used as photocatalyst to decompose MO as probe pollutant in aqueous solution. XRD and EDAX analysis didn't show any peaks to confirm the appearance of unwanted impurities. SEM analysis confirmed that all samples are uniform, global and slightly agglomerated and TEM analysis confirmed the results diagnosed from SEM and XRD analysis. The photocatalytic activity of pure TiO_2 is greatly improved in presence of loaded metal nanoclusters with 0.2% In and 0.2% V content. The high visible-light-driven photocatalytic activity of In and V modified TiO_2 is ascribed to the synergetic effects of (1) decreased particle size; (2) improved visible-light harvesting ability due to formation of sub-energy levels in TiO_2 structure, and (3) increased efficiency in separation of photo-generated charge carriers. This investigation contributes to the understanding effects of the complex ion doping on TiO_2 photoactivity and thus, provides a reference for improving its environmental application.

Acknowledgements

We are grateful to Council of University of Kashan, Iran Nanotechnology Initiative Council and The University of Texas at El Paso (UTEP) for providing financial support. We also thank Dr. Peter Cooke from New Mexico State University (NMSU) for helping us with TEM measurements, Dr. Jing Wu from Texas A&M University for helping us with XPS analysis, Dr. Juan Noveron from chemistry department of UTEP for providing us with UV light reactor, and the College of Engineering at UTEP for allowing access to their SEM, EDAX and XRD instruments.

References

1 K. Chen, J. Li, J. Li, Y. Zhang, W. Wang, Colloids and Surfaces A: Physicochem. Eng., 2010, **360**, 47.
2 X. Xiao, K. Ouyang, R. Liu, J. Liang, Applied Surf. Sci. 2009, **255**, 3659.
3 L. Armelao, D. Barreca, Nanotech. 2007, **18**, 375709.
4 S. Watson, D. Beydoun, J. Scott, R. Amal, J. of Nanoparticle Research, 2004, **6**, 193.
5 S. Xu, Y. Zhu, L. Jiang, Y. Dan, Water Air Soil Pollut., 2010, **213**, 151.
6 E. Khelifi, H. Gannoun, Y. Touhami, H. Bouallagui, M. Hamdi, Journal of Hazardous Materials, 2008, **152**, 683.
7 S. Kim, S. Hwang, W. Choi, J. Phys. Chem. B, 2005, **109**, 24260.
8 O. Rosseler, M. Shankar, K-L. DuM, L. Schmidlin, N. Keller, V. Keller, J. Catal., 2010, **269**, 179.
9 M. Hamadanian, S. Karimzadeh, V. Jabbari, D. Villagrán, Materials Science in Semiconductor Processing, 2015, Accepted.
10 N. Murakami, T. Chiyoya, T. Tsubota, T. Ohno, Appl, Catal. A, 2008, **348**, 148.
11 L. G. Devi, B. N. Murthy, S. G. Kumar, Mater Sci Eng. B, 2010, **166**, 1.
12 M. Hamadanian, A. S. Sarabi, A. Mihammadi Mehra, V. Jabbari, Applied Surface Science, 2011, **257**, 10639.
13 V. Jabbari, M. Hamadanian, M. Shamshiri, Applied Surface Science, 2014, **317**, 302.
14 D. M. Chen, D. Yang, Q. Wang, Z. Y. Jiang, Ind. Eng. Chem. Res., 2006, **45**, 4110.
15 O. Carp, C. L. Huisman, A. Reller, Prog. Solid. State. Chem., 2004, **32**, 33.
16 H. S. Hilal, L. Z. Majjad, N. Zaatar, A. El-Hamouz, Solid. State. Sci. 2007, **9**, 9.
17 D. Jiang, Y. Xu, B. Hou, D. Wu, Y. J. Sun, Solid State Chem., 2007, **180**, 1787.
18 B. Liu, X. Zhao, N. Zhang, Q. Zhao, X. He, J. Feng, Surf. Sci., 2005, **595**, 203
19 Dawson, P. V. Kamat, J. Phys. Chem., 2001, **105**, 960.
20 Molinari, R. Amadelli, L. Antolini, A. Maldatti, P. Battioni, D. Mansuy, J. Mol. Catal. A: Chem., 2000, **158**, 521.
21 D. Bahnemann, A. Henglein, J. Lilie, L. Spanhel, J. Phys. Chem., 1984, **88**, 709.
22 O. V. Makarova, T. Rajh, M. C. Thurnauer, A. Martin, P. A. Kemme, D. Cropek, Environ. Sci. Technol., 2000, **34**, 4797.
23 D. Raftery, S. Klosek, J. Phys. Chem. B, 2001, **105**, 2815.
24 J.C.-S. Wu, C.H. Chen. J Photochem Photobiol A, 2004, **163**, 509.
25 W.Y. Choi, A. Termin, M.R. J. Hoffmann, Phys. Chem., 1994, **98**, 13669.
26 E. Wang, W. Yang and Y. Cao, J. Phys. Chem. C, 2009, **113**, 20912.
27 Liu, X. Zhao, N. Zhang, Q. Zhao, X. He, J. Feng, Surf. Sci., 2005, **595**, 203.
28 R. Estrellan, C. Salim, H. Hinode, Journal of Hazardous Materials, 2010, **179**, 79.
29 N. Serpone, J. Phys. Chem. B, 2006, **110**, 24287.
30 R. Zhang, Y. H. Kim, Y. S. Kang, Curr. Appl. Phys., 2006, **6**, 801.
31 S. Dong, C. Tang, H. Zhou, H. Zhao, Gold Bulletin, 2004, **37**, 3.
32 M. Hamadanian, A. Reisi-Vanani, A. Majedi, Materials Chemistry and Physics, 2009, **116**, 376.
33 J. H. Kim, B. H. Noh, G. D. Lee, S. S. Hong, Korean J. Chem. Eng, 2005, **22**, 370.
34 Li, H. Haneda, S. Hishita, N. Ohashi, Chem. Mater., 2005, **17**, 2588.
35 Jun Zhang, Junhua Xiab and Zhenguo Ji, J. Mater. Chem. 2012, **22**, 17700.
36 M. Hamadanian, M. Amani, V. Jabbari, Polymer-Plastics Technology and Engineering, 2014, **53**, 1283.
37 Wu-Qiang Wu, Hua-Shang Rao, Yang-Fan Xu, Yu-Fen Wang, Cheng-Yong Su & Dai-Bin Kuang, Scientific Reports, 2013, **3**, 1892
38 Jiao Li, Junbo Xu and Jianguo Huang, CrystEngComm, 2014, **16**, 375.
39 Jiayong Gan et al., Scientific Reports, 2013, **3**, 1021.
40 Reddy, L. Davydov, P. Smirniots, J. Phys. Chem. B, 2002, **106**, 3394.

41 X. Yang, L. Xu, X. Yu, Y. Guo, Catalysis Communications, 2008, **9**, 1224.
42 J. Xie, X. Lu, M. Chen, G. Zhao, Y. Song, S. Lu, Dyes and Pigments, 2008, **77**, 43.
43 Mills, M. McGrady, Journal of Photochemistry and Photobiology A: Chemistry, 2008, **193**, 228.
44 J. Zhu, W. Zheng, B. He, J. Zhang, M. Anpo, J. Mol. Catal. A: Chem., 2004, **216**, 35.